Suppression of electron relaxation and dephasing rates in quantum dots caused by external magnetic fields

Suppression of electron relaxation and dephasing rates in quantum dots caused by external magnetic fields

V N Stavrou

Department of Physics, State University of New York at Buffalo, NY 14260, USA
and
Department of Physics and Astronomy, University of Iowa, Iowa City, IA 52242, USA

Abstract
An external magnetic field has been applied in laterally coupled quantum dots
(QDs) and we have studied the QD properties related to charge decoherence.
The significance of the applied magnetic field to the suppression of electron–
phonon relaxation and dephasing rates has been explored. The coupled QDs
have been studied by varying the magnetic field and the interdot distance as
well as other system parameters. Our numerical results show that the electron
scattering rates are strongly dependent on the applied external magnetic field
and the details of the double QD configuration.

1. Introduction

Relaxation and decoherence properties in electronic devices such as low-dimensional structures
and specifically in quantum dots (QDs) have attracted the interest of experimental and
theoretical studies. Fabricated coupled QDs have been suggested as candidates for quantum
bits (qubits) where the states of a single trapped electron within the coupled QDs can perform
the two states of the qubit [1–6]. The investigated devices are mainly characterized by two
important decoherence channels. The first one is the coulomb interaction to the background
charge fluctuation which is an extrinsic decoherence and the second channel, an intrinsic
decoherence, due to electron–phonon interaction. The theoretical studies of the above-
mentioned intrinsic decoherence due to single electron–phonon coupling are mainly related
to the single phonon emission process. Although the electron relaxation through multi phonon
processes is an important parameter at high temperature, at the qubit operation temperature
($\sim$1 T) these processes do not have strong effects [7].

It is worth mentioning that during the last decade a vast amount of research has been
published on double QDs dephasing [8]. In our previous work [9], we reported the results
of charge decoherence due to relaxation and dephasing rates caused by electron–phonon
interaction. In the present investigation, we report the significance of longitudinal acoustic
(LA) phonons (including the deformation and piezoelectric interactions) and LO phonons on
relaxation and dephasing rates in laterally coupled QDs under the existence of magnetic fields.

The existence of an external magnetic field is of special importance for the electron states [10] due to the decrease of electron energy splitting as the magnetic field increases. The scattering rates have been found to depend strongly on electron confinement and the interdot distance. Acoustic phonons are only used in the calculations of the relaxation rate due to the small electron energy splitting ($\leqslant 1$ meV). For the dephasing rates, both the acoustic and optical phonons are considered.

The paper is organized as follows. In section 2, we describe the electron wavefunctions in the presence of an external magnetic field and the models for the acoustical and optical phonon modes. In section 3, we outline the scattering theory of an electron which is scattered to an energetically smaller state by the emission of acoustical phonons. The dephasing rates have been also studied by considering the emission of acoustical and optical phonons. Section 4 is devoted to the numerical results and interpretation of suppression of decoherence due to magnetic field. Lastly, section 5 presents a summary of the present work.

2. The models of charge qubit and phonons

2.1. Electron wavefunctions

We consider a single electron within two coupled identical QDs with an interdot distance 2α. The lateral electron motion is decoupled from the one along the QW growth [11]. The Hamiltonian which describes the single electron motion which is confined in laterally coupled QDs is given by

$$\hat{\mathcal{H}} = \hat{\mathcal{H}}_{\parallel} + \hat{\mathcal{H}}_z \tag{1}$$

where the QW growth is denoted by the subscript 'z' and the lateral direction by '$\parallel$'.

The external magnetic field enters the Hamiltonian via a magnetic vector potential **A**. By choosing the symmetric gauge $\mathbf{A} = \mathcal{B}(-y\hat{\mathbf{e}}_{\mathbf{x}} + x\hat{\mathbf{e}}_{\mathbf{y}})/2$ then the magnetic field points to z direction and it is given by $\mathbf{B} = \nabla \times \mathbf{A} = \mathcal{B}\hat{\mathbf{e}}_{\mathbf{z}}$. The lateral confinement is assumed to be parabolic for a single QD, therefore, the Hamiltonian operator for the lateral directions has been considered as [10]

$$\hat{\mathcal{H}}_{\parallel} = \frac{\hat{p}^2}{2m^*} + \frac{1}{2}m^*\omega^2 r_{\parallel}^2 - \frac{1}{2}\omega_c \mathbf{L}_z \tag{2}$$

where the operator of the z component of the angular momentum is given by

$$\mathbf{L_z} = -\mathrm{i}\hbar\left[-y\frac{\partial}{\partial x} + x\frac{\partial}{\partial y}\right] \tag{3}$$

with $\hat{p}$ the quantum mechanical operator of momentum, ω_0 is a parameter (in this case frequency) describing the strength of the confinement in the x–y plane, $\omega_c = \mathcal{B}e/m^*$, and $\omega^2 = \omega_0^2 + (\omega_c/2)^2$. The electron wavefunction can be separated into the following envelope functions,

$$\psi(\mathbf{r}) = \psi_{\parallel}\left(\mathbf{r}_{\parallel}\right)\psi_z(z). \tag{4}$$

In the case of a single QD, the one electron wavefunction can be given in terms of the principal quantum number n ($n = 0, 1, 2, \ldots$) and the angular momentum quantum number m ($m = 0, \pm 1, \pm 2, \ldots$) as

$$\psi_{\parallel}^{(n,m)}(\tilde{\rho}, \theta) = \sqrt{\frac{n!}{\pi l^2(n+|m|)!}}\,\tilde{\rho}^{|m|}\mathrm{e}^{-\tilde{\rho}^2/2}\mathrm{e}^{\mathrm{i}m\theta}\mathcal{L}_n^{|m|}\left(\tilde{\rho}^2\right) \tag{5}$$

where $\mathcal{L}_n^{|m|}\left(\tilde{\rho}^2\right)$ are the Laguerre polynomials, and $\tilde{\rho}$ is a scaled radius, $\tilde{\rho} = \mathbf{r}_{\parallel}/l$, with $l = \sqrt{\hbar/m^*\omega_0}$. The eigenvalues of the single particle are given by

$$E_{nm} = (2n + |m| + 1)\,\hbar\omega_0. \tag{6}$$

By using the Heaviside step function Θ, the Hamiltonian, along the QW growth, takes the form

$$\hat{\mathcal{H}}_z = -\frac{\hbar}{2}\partial_z\frac{1}{m^*(z)}\partial_z + V_0\Theta\left(|z| - L_z\right) \tag{7}$$

where $m^*(z)$ is the electron effective mass and V_0 the offset between the band edges well and barrier. The wavefunction along the above-mentioned direction has been considered as the wavefunction of an infinite QW ($V_0 \to \infty$). Here, it has been used only for the ground state wavefunction along the QW growth due to the strong confinement along this direction. The ground state wavefunction is given by $\psi_z(z) = \mathcal{A}\cos(\pi z/2L_z)$ where $\mathcal{A}$ is a coefficient to be determined by normalization and $2L_z$ is the size of the QW.

The wavefunction of a single electron, which is confined in a 2D QD and is coupled in one dimension of the $x-y$ plane, can be formed by superposition of two uncoupled QDs which are sited 'left' and 'right' of the origin of the frame of reference and are separated by an inter-dot distance 2α. The external confining potential which is used is given by

$$V_c = \tfrac{1}{2}m^*\omega_0^2\min\{(x - \alpha)^2 + y^2, \ (x + \alpha)^2 + y^2\}. \tag{8}$$

The single electron wavefunction for the parallel plane can be given by:

$$\left|\Psi_{\parallel}\right\rangle = \sum_k C_k\left|\psi_{\parallel,L}^k\right\rangle + D_k\left|\psi_{\parallel,R}^k\right\rangle \tag{9}$$

and the total wavefunction of the system of coupled QDs as described above is

$$\Psi(\mathbf{r}) = \Psi_{\parallel}\left(\mathbf{r}_{\parallel}\right)\psi_z\left(z\right). \tag{10}$$

The wavefunctions in the parallel plane of the coupled QDs system are calculated numerically by direct diagonalization.

2.2. Acoustic and optical phonons

The electrons, in polar semiconductors, couple to acoustical and optical phonons. The small electron energy splitting does not permit any electron transition in the charge qubit via the emission of optical phonons. On the other hand, the acoustical phonons contribute to the relaxation rates due to the small phonon energies. Here, we calculate the decoherence rates which are caused by deformation potential and piezoelectric acoustic phonon interaction by considering only longitudinal phonons. It follows that the Hamiltonian which describes these interactions [12]:

$$H = \sum_{\mathbf{q}}\left(\frac{\hbar}{2\rho_m V\omega_{\mathbf{q}}}\right)^{1/2}\mathcal{M}(\mathbf{q})\rho(\mathbf{q})(a_{\mathbf{q}} + a_{-\mathbf{q}}^{\dagger}), \tag{11}$$

where $\omega_{\mathbf{q}}$ is the frequency of the phonon mode with wavevector $\mathbf{q}$, ρ_m is the mass density of the host material, V is the volume of the sample, $a_{\mathbf{q}}$ and $a_{-\mathbf{q}}^{\dagger}$ are phonon annihilation and creation operators, and $\rho(\mathbf{q})$ is the electron density operator. The term $\mathcal{M}(\mathbf{q})$ is given by

$$\mathcal{M}(\mathbf{q}) = D|\mathbf{q}| + \mathrm{i}\mathcal{M}_{\lambda}(\hat{q}) \tag{12}$$

The first term of the above equation represents the deformation potential interaction with deformation potential D and the second part, which is imaginary, is the piezoelectric interaction [13]. For zincblende crystals (e.g. GaAs), the term $\mathcal{M}_{\lambda}(\hat{q})$ can have the form [14]

$$\mathcal{M}_{\lambda}^{pz}(\hat{\mathbf{q}}) = 2e\,e_{14}\left(\hat{q}_x\hat{q}_y\xi_z + \hat{q}_y\hat{q}_z\xi_x + \hat{q}_x\hat{q}_z\xi_y\right) \tag{13}$$

where e is the electronic charge, e_{14} is the piezoelectric constant, and ξ is the unit polarization vector.

The fact that the energy difference between the electron states in coupled quantum dots is quite small (a few meV) does not allow optical phonon transitions due to the conservation of energy (optical phonon energy is $\sim$36 meV in GaAs). The optical phonons play a role in dephasing rates as we demonstrate in the next section. By using the bulk phonon approximation and neglecting the interface phonon modes [15, 16], the electron–phonon interaction due to LO phonons is thus given by [12]

$$H_{\text{OP}} = \sum_{\mathbf{q}} \frac{M}{q\sqrt{V}} \rho(\mathbf{q}) (a_{\mathbf{q}} + a_{-\mathbf{q}}^{\dagger}) \tag{14}$$

and

$$M^2 = 2\pi e^2 \hbar \omega_{\text{LO}} \left(\frac{1}{\epsilon_{\infty}} - \frac{1}{\epsilon_{\text{s}}} \right) \tag{15}$$

where ω_{LO} is the longitudinal optical frequency, ϵ_{s} and ϵ_{∞} are the static and high frequency dielectric constants of the host material.

Having described the electronic states in coupled QDs and the relevant types of phonon, we are now ready to calculate the relaxation and dephasing rates. The next section is devoted to Fermi's golden rule and dephasing rates.

3. Theory of relaxation and dephasing rates

The relaxation rate between an initial $|\Psi^{(\text{I})}\rangle$ and a final state $|\Psi^{(\text{F})}\rangle$ associated with phonon emission $(+)$ (or absorption $(-)$) is determined by Fermi's golden rule:

$$\Gamma = \frac{2\pi}{\hbar} \sum_{\mathbf{q}} \left| \langle \Psi^{(\text{F})}(\mathbf{r}) \left| H^{\text{int}} \right| \Psi^{(\text{I})}(\mathbf{r}) \rangle \right|^2 \delta \left(E_{\text{F}} - E_{\text{I}} \pm E_{\mathbf{q}} \right) \left(N_{\text{B}}(E_{\mathbf{q}}, T_{\text{lat}}) + \frac{1}{2} \pm \frac{1}{2} \right) \tag{16}$$

where the labels 'I' and 'F' denote the initial and final electron states respectively. N_{B} is the Bose–Einstein distribution function for phonons with lattice temperature T_{lat}. It is worth mentioning that in our calculations we assumed $T_{\text{lat}} = 0$ and the phonon absorption can be neglected.

It is also worth mentioning that relaxation is not the only way charge qubits can be decohered. If the energy difference between the two charge states fluctuates, phase information will become lost and decoherence occurs. The density operator of an electron in a boson bath is given in [17, 18]

$$\rho(t) = \begin{pmatrix} \rho_{00}(0) & \rho_{01}(0) e^{-B^2(\Delta t) + i\varepsilon \Delta t/\hbar} \\ \rho_{10}(0) e^{-B^2(\Delta t) - i\varepsilon \Delta t/\hbar} & \rho_{11}(0) \end{pmatrix} \tag{17}$$

where ε is the energy splitting between the electron energy levels. In short, pure dephasing causes a decay in the off-diagonal element of the density matrix for the two-level system that makes up the charge qubit [17, 18]:

$$\rho_{01}(t) \sim \rho_{01}(0) e^{-B^2(t)}, \tag{18}$$

where the exponent function $B^2(t)$ is defined by

$$B^2(t) = \frac{V}{\hbar^2 \pi^3} \int \text{d}^3 \mathbf{q} \, \frac{|g(\mathbf{q})|^2}{\omega_{\mathbf{q}}^2} \sin^2 \frac{\omega_{\mathbf{q}} t}{2} \coth \frac{\hbar \omega_{\mathbf{q}}}{2 k_{\text{B}} T}. \tag{19}$$
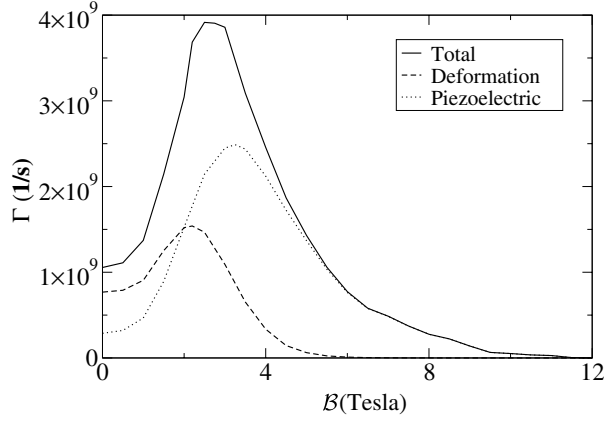
Figure 1. Relaxation rates of an electron, which scatters from the first excited state to the ground state, versus the external magnetic field. The confinement strength is $\hbar\omega_0 = 3$ meV, half the interdot distance $\alpha = 20$ nm and QW width $2L_z = 10$ nm.

For acoustic phonons, we choose frequencies $\omega_{\mathbf{q}} = qc_s$ for the relevant branches, while for longitudinal optical phonons, we choose $\omega_{\mathbf{q}} = \omega_{\mathrm{LO}}$. The coupling constants $g(\mathbf{q})$ due to deformation potential, piezoelectric, and optical phonons are respectively given by

$$g_{\mathrm{def}}(\mathbf{q}) = D\sqrt{\frac{\hbar q}{2\rho c_s V}}\mathcal{I}(\mathbf{q}), \tag{20}$$

$$g_{\mathrm{piezo}}(\mathbf{q}) = \mathcal{M}_\lambda^{pz}(\mathbf{q})\sqrt{\frac{\hbar}{2\rho c_s V}}\mathcal{I}(\mathbf{q}), \tag{21}$$

$$g_{\mathrm{polar}}(\mathbf{q}) = \frac{M}{q\sqrt{V}}\mathcal{I}(\mathbf{q}), \tag{22}$$

where $\mathcal{I}(\mathbf{q})$ is given by

$$\mathcal{I}(\mathbf{q}) = \tfrac{1}{2}\left(\left\langle\Psi^-(\mathbf{r})\left|e^{\mp i\mathbf{q}\cdot\mathbf{r}}\right|\Psi^-(\mathbf{r})\right\rangle - \left\langle\Psi^+(\mathbf{r})\left|e^{\mp i\mathbf{q}\cdot\mathbf{r}}\right|\Psi^+(\mathbf{r})\right\rangle\right) \tag{23}$$

the symbols ($\pm$) refer to the two states for the double dot charge qubit. The matrix integrals in this study are carried out using the Monte Carlo algorithms.

4. Results and discussions

We firstly calculate the relaxation rates as a function of an external magnetic field $\mathcal{B}$, for an electron which scatters from the first excited to the ground state associated with the emission of acoustical phonons. In all our calculations, the quantum well width is fixed to the value of $2L_z = 10$ nm and the confinement lengths in the x an y directions are 0.5 μm.

As it appears in figure 1, for small magnetic field the relaxation rates due to deformation interaction are larger than those due to piezoelectric interaction. As the field $\mathcal{B}$ increases, the piezoelectric coupling becomes the dominate contributor due to the different wavevector dependence in the deformation and piezoelectric matrix elements. For the deformation potential, the dependence of matrix elements on wavevector is related to $\sqrt{q}$ while for the piezoelectric coupling it is related to $1/\sqrt{q}$. The relaxation rates for small magnetic field increase up to a maximum value and afterwards decrease. This resonance reflects the existence of large electron wavefunctions of the charge qubit (for $\mathcal{B} \approx 3$ T).
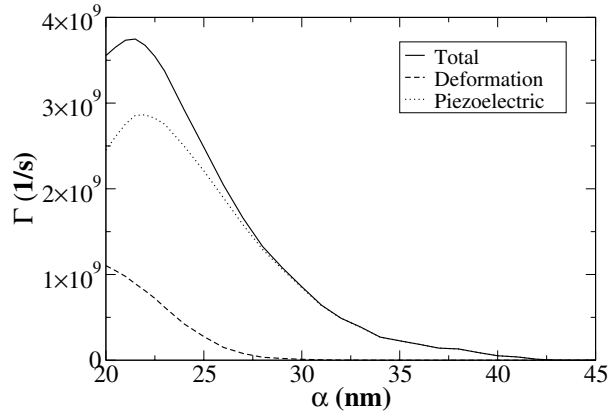
Figure 2. Relaxation rates of an electron versus half the interdot distance α. The confinement strength is $\hbar\omega_0 = 3$ meV, the magnetic field $\mathcal{B} = 3$ T, and QW width $2L_z = 10$ nm.
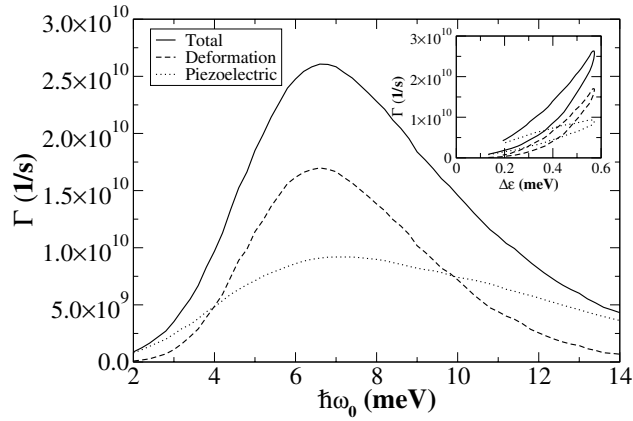

Figure 3. Relaxation rates of an electron versus the strength of the confinement $\hbar\omega_0$. Electron relaxation rates as a function of the energy splitting between the first excited state and the ground state are given in the inset. Half the interdot distance is $\alpha = 20$ nm, magnetic field $\mathcal{B} = 3$ T, and QW width $2L_z = 10$ nm.

Figure 2 presents the electron relaxation rates as a function of half the interdot distance for a fixed $\mathcal{B} = 3$ T and $\hbar\omega_0 = 3$ meV. As the interdot distance increases the rates decrease due to the small energy splitting which results in a small phonon density of states. Thus the relaxation rates become small as the interdot distance increases. For α close to 21.5 nm, it is obvious that the rates get a maximum value due to large wavefunctions. The different dependence of matrix elements on the phonon wavefunction for the deformation potential and piezoelectric interaction results in the different behaviour of the relaxation rates for the above-mentioned interactions.

The dependence of the relaxation rates on the electron confinement strength is shown in figure 3. The rates increase as the energy splitting between the first excited and ground state increases. When the electron strength of the electron confinement reaches the value $\hbar\omega_0 = 6.5$ meV, the relaxation rates get a maximum value. Increasing the electron confinement strength, the energy splitting becomes small and the relaxation rates decrease as a consequence
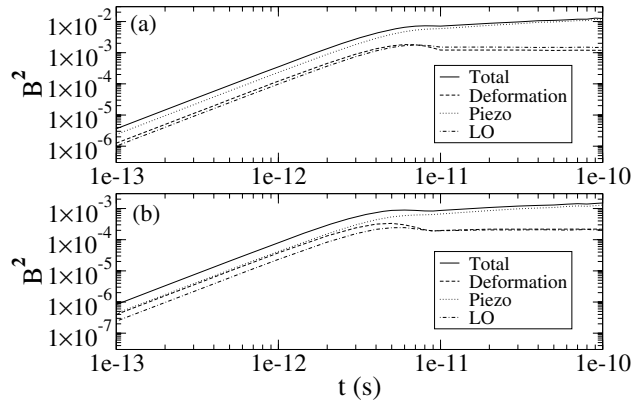
Figure 4. Dephasing factor $B^2(t)$ as a function of time t. The dephasing factor due to deformation potential, piezoelectric interaction, LO and the total rates are represented by dashed, dotted, dashed–dotted, and straight lines respectively. The strength of the confinement is $\hbar\omega_0 = 3$ meV, half the interdot distance is $\alpha = 20$ nm, with (a) $\mathcal{B} = 0$ T and (b) $\mathcal{B} = 3$ T.

of the energy splitting degradation. The dependence of relaxation rates on the energy splitting is shown in the inset in figure 3. This reflects the fact that for a given energy splitting, there are two corresponding values of the strength of the confinement [9]. As a result there are two values of relaxation rates for each energy splitting. The two different types of electron–phonon interactions produce different contributions to the total relaxation rates and can be interpreted in the same manner as in figure 1.

The second part of our investigation of decoherence in charge qubits is the evaluation of dephasing factor and its dependence on an external magnetic field. Here, we calculate the dephasing effects from both acoustic (deformation, piezoelectric) and optical phonons. Figure 4 shows the temporal dependence for two different values of an external magnetic field. The curves in figure 4 rapidly increase for the first 10 ps and for later times they saturate. As a result $B^2(t)$ depends only very slowly on time after 100 ps. The interaction between the qubit electron and the acoustic phonon bath causes the fast increase of dephasing in a period of time less than 100 ps. Mathematically, the very fast time dependence of dephasing is due to the trigonometric dependence on phonon frequencies and time (see [9]). For larger time is practically flat and can be considered constant after 100 ps. A constant dephasing factor will not produce a decaying signal in terms of, for example, oscillations in electrons. Instead, it simply reduces the contrast in the charge oscillation. This can be seen easily from equation (17). The presence of a constant $\exp(-B^2) \sim \exp(-0.05)$ simply reduces the magnitude of ρ_{01} by a constant factor of 0.05, which is not a particularly large suppression (though significant in terms of fault tolerant quantum computing).

The temporal behaviour of the dephasing factor has an interesting feature for zero and a non-zero magnetic field. $B^2(t)$ decreases as $\mathcal{B}$ increases (figures 4(a) and (b)) due to the dependence of the matrix elements on the initial and final wavefunctions in the presence of an external magnetic field. Figure 5 shows the dephasing rates as a function of an external magnetic field. As the field $\mathcal{B}$ increases, the quantity $\mathcal{I}(\mathbf{q})$ in equation (23) decreases as a consequence of the smaller differences in the matrix elements involved in equation (23). For large magnetic fields the rates go to zero.

Finally, we calculate the dephasing rates as a function of half the interdot distance for a fixed external magnetic field and electron confinement strength (figure 6). As in the case of the
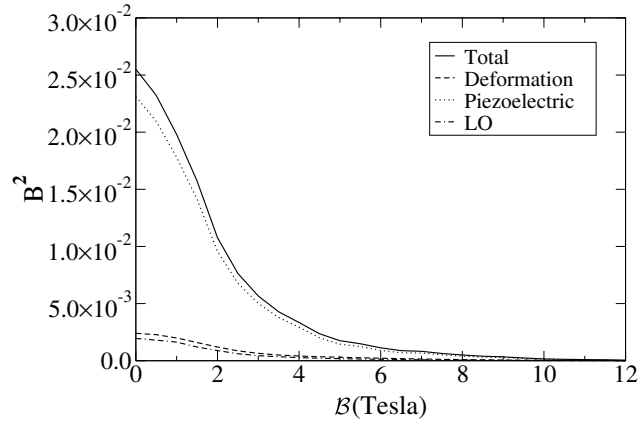
Figure 5. Dephasing factor $B^2(t)$ as a function of the magnetic field. The time t is chosen to be 60 ps. The solid line represents dephasing rates due electron–acoustic phonon interactions. The dephasing rates due to deformation potential, piezoelectric interaction and polar interaction with optical phonons are represented by dashed, dotted, and dash–dotted lines respectively. The strength of the confinement is $\hbar\omega_0 = 3$ meV. Half the interdot distance $\alpha = 20$ nm and QW width $2L_z = 10$ nm.
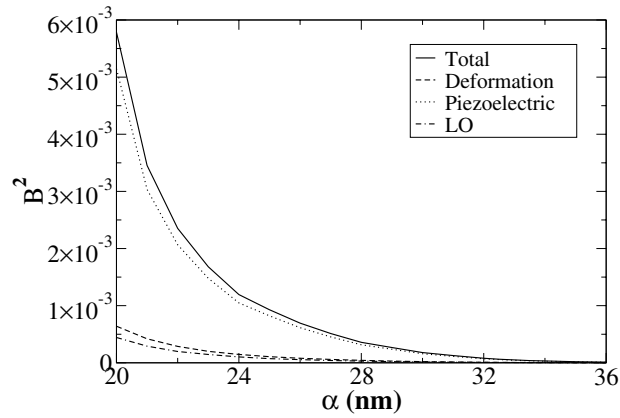

Figure 6. Dephasing factor $B^2(t)$ as a function of the half interdot distance α. The time t is chosen to be 60 ps. The solid line represents dephasing rates due to electron–acoustic phonon interactions. The dephasing rates due to deformation potential, piezoelectric interaction and polar interaction with optical phonons are represented by dashed, dotted, and dash–dotted lines respectively. The strength of the confinement is $\hbar\omega_0 = 3$ meV. $\mathcal{B} = 3$ T and QW width $2L_z = 10$ nm.

relaxation rates, the dephasing rates decrease by increasing the interdot distance due to the fact that when the two QDS are well separated then the integral difference in equation (23) goes down quickly. Consequently, the dephasing factor $B^2(t)$ undergoes suppression by increasing the separation distance.

5. Conclusions

We have studied the phonon-induced single electron relaxation and dephasing rates in laterally coupled QDs in the presence of an external magnetic field. The relaxation and dephasing

rates have been calculated for different system parameters such as interdot distance, strength of electron confinement and magnetic field. In the case of zero magnetic field [9], the rates could be enhanced for some double dot configurations. This enhancement of the rates could be easily suppressed by the existence of an external magnetic field. Our results show that the magnetic field is of crucial importance in the study of the decoherence in charge qubits due to the suppression of electron relaxation and dephasing rates.

Acknowledgments

References

[1] Barenco A, Deutsch D, Ekert A and Jozsa R 1995 *Phys. Rev. Lett.* **74** 4083
[2] Ekert A and Josza R 1996 *Rev. Mod. Phys.* **68** 733
[3] Sherwin M S, Imamoglu A and Montroy T 1999 *Phys. Rev.* A **60** 3508
[4] Tanamoto T 2000 *Phys. Rev.* A **61** 022305
[5] Larionov A A, Fedichkin L E and Valiev K A 2001 *Nanotechnology* **12** 536
[6] Hollenberg L C L, Dzurak A S, Wellard C, Hamilton A R, Reilly D J, Milburn G J and Clark R G 2004 *Phys. Rev.* B **69** 113301
[7] Stavrou V N and Hu X 2006 *Phys. Rev.* B **73** 205313
[8] Machnikowski P 2006 *Phys. Rev. Lett.* **96** 140405 and references therein
[9] Stavrou V N and Hu X 2005 *Phys. Rev.* B **72** 075362
[10] Jacak L, Hawrylak P and Wójs A 1998 *Quantum Dots* (Berlin: Springer)
[11] Bockelmann U 1994 *Phys. Rev.* B **50** 17271
[12] Mahan G D 1990 *Many-Particle Physics* (New York: Plenum)
[13] Mahan G D 1972 *Polarons in Ionic Crystals and Polar Semiconductors* ed J T Devreese (Amsterdam: North-Holland) pp 553–657
[14] Bruus H, Flensberg K and Smith H 1993 *Phys. Rev.* B **48** 11144
[15] Constantinou N C 1991 *J. Phys.: Condens. Matter* **3** 6859
     Stavrou V N, Babiker M and Bennett C R 2001 *J. Phys.: Condens. Matter* **13** 6489
     Stavrou V N, Bennett C R, Al-Dossary O M M and Babiker M 2001 *Phys. Rev.* B **63** 205304
     Stavrou V N 2003 *Physica* B **337** 87
[16] Ridley B K 1996 *Electrons and Phonons in Semiconductors* (Cambridge: Cambridge University Press)
[17] Palma G M, Suominen K A and Ekert A K 1996 *Proc. R. Soc. Lond.* A **452** 567–84
[18] Duan L M and Guo G C 1998 *Phys. Rev.* A **57** 737